Ultracold atom-ion collisions

R. Côté[1] and A. Dalgarno[2]
[1]*Physics Department, University of Connecticut, 2152 Hillside Road, Storrs, Connecticut 06269-3046*
[2]*Institute for Theoretical Atomic and Molecular Physics (ITAMP), Center for Astrophysics, 60 Garden Street, Cambridge, Massachusetts 02138*

(Received 4 February 2000; published 14 June 2000)

Studies of charge transfer and total cross sections in elastic collisions of atom-ion alkali metals at ultralow temperatures are reported. Calculations for $Na+Na^+$ have been carried out with the best available $^2\Sigma_g^+$ and $^2\Sigma_u^+$ potential curves. As functions of energy, the cross sections show considerable structure and are large in the limit of low temperature. The scattering lengths were also computed, and the effective range expansion verified. For higher temperatures, we compare quantal and semiclassical results, and investigate the range of applicability of the Langevin formula. Even at temperatures of a few degrees kelvin, the charge-transfer cross sections are large, and could provide an efficient way to produce cold ions.

PACS number(s): 34.10.+x, 34.20.−b, 34.50.−s, 34.70.+e

I. INTRODUCTION

Collisions of atoms at ultracold temperatures have received considerable attention because of their importance in the cooling and trapping of atoms [1] and molecules [2] and their role in high precision spectroscopy [3] and Bose-Einstein condensation [4]. Neutral-atom collisions at ultracold temperatures may be characterized by *s*-wave scattering lengths. Collisions of ions and atoms involve higher-order partial waves because of the long-range attractive polarization forces and differ also because of the possibility of charge transfer. The cross sections may be large and charge transfer between ions and atoms will occur with high efficiency. Ion-atom collisions influence the behavior of plasmas and determine the magnitude of the ion mobilities and diffusion coefficients. An ultracold plasma of xenon has been created [5] and similar techniques may be used to create alkali-metal plasmas [6].

In this paper we explore the neutral-atom–ion-collision properties in the ultralow-energy regime. We calculate the elastic and charge-transfer cross sections using accurate potential curves. We determine the elastic scattering lengths for the $^2\Sigma_g^+$ and $^2\Sigma_u^+$ states of Na_2^+, and verify the effective range expansion for the *s*-wave contribution. We examine the contribution of higher partial waves to the cross sections. The charge-transfer and diffusion cross sections are computed using a quantal treatment, and are shown to be well described by a simple semiclassical model. We compute the ion diffusion coefficient and mobility. The mobility follows a simple classical expression for temperatures ranging from 10 nK to 100 K. Below 10 nK, we predict a rapid increase of the mobility with decreasing temperature.

II. PROCESSES

We study the collision between an ion and its neutral parent atom. Although we use $Na+Na^+$ as an example, many of our conclusions apply to other alkali-metal ion-atom collisions. A neutral atom of Na collides elastically with Na^+ in the $^2\Sigma_g^+$ or $^2\Sigma_u^+$ states of Na_2^+. The elastic collision may be represented by

$$Na+Na^+ \rightarrow \left\{ \begin{array}{c} Na_2^+(^2\Sigma_g^+) \\ \text{or} \\ Na_2^+(^2\Sigma_u^+) \end{array} \right\} \rightarrow Na+Na^+.$$

The elastic cross section is given by [7]

$$\sigma_{\text{el.}} = \frac{1}{2}[\sigma_{\text{el.}}^g + \sigma_{\text{el.}}^u], \tag{1}$$

with

$$\sigma_{\text{el.}}^{g,u} = \frac{4\pi}{k^2} \sum_{l=0}^{\infty} (2l+1)\sin^2(\eta_l^{g,u}), \tag{2}$$

where $k=\sqrt{2\mu E}/\hbar$ with μ the reduced mass and E the collision energy in the center-of-mass system, and $\eta_l^{g,u}$ is the lth partial-wave phase shift corresponding to the $^2\Sigma_g^+$ and $^2\Sigma_u^+$ states, respectively. Another possible outcome is charge transfer,

$$Na+Na^+ \rightarrow \left\{ \begin{array}{c} Na_2^+(^2\Sigma_g^+) \\ \text{and} \\ Na_2^+(^2\Sigma_u^+) \end{array} \right\} \rightarrow Na^+ + Na.$$

The charge-transfer cross section is given by [7]

$$\sigma_{\text{ch.}} = \frac{\pi}{k^2} \sum_{l=0}^{\infty} (2l+1)\sin^2(\eta_l^g - \eta_l^u). \tag{3}$$

For the two doublet potential-energy curves $^2\Sigma_g^+$ and $^2\Sigma_u^+$, we used the *ab initio* data of Magnier [8], ranging from 5.0 to 20.0 bohr radii a_0, extended to large distances by the asymptotic form

$$V_{g,u}(R) \sim V_{\text{disp.}}(R) \mp V_{\text{exch.}}(R) \tag{4}$$

with $\mp$ for g and u, respectively. The dispersion term is given, in atomic units, by

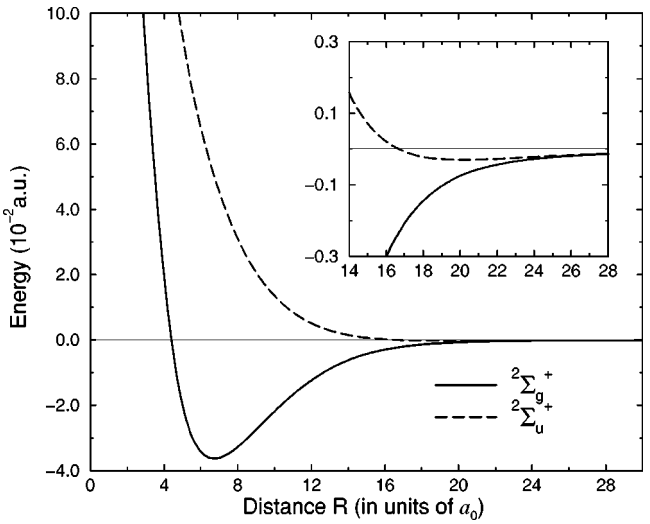

FIG. 1. The two lowest potential curves for Na_2^+. The inset shows an enlarged energy scale.

$$V_{\text{disp.}}(R) = -\frac{1}{2}\left[\frac{C_4}{R^4} + \frac{C_6}{R^6} + \frac{C_8}{R^8}\right], \tag{5}$$

with $C_4 = 162.7$, $C_6 = 1873.0$, and $C_8 = 54\,139.0$. The coefficient C_4 is the dipole polarizability of the sodium atom [9]. The coefficient C_6 is the quadrupole polarizability of Na, 1849.0 a.u. [10], to which we added the estimate of 24.0 a.u. for the relatively small contribution of the ion-atom Na^+-Na van der Waals interaction. The coefficient C_8 is the octupole polarizability of Na [10]. The exchange term was found using the treatment of Bardsley *et al.* [11] and takes the form, in atomic units,

$$V_{\text{exch.}}(R) = \frac{1}{2} A R^{\alpha} e^{-\beta R}\left[1 + \frac{B}{R} + O\left(\frac{1}{R^2}\right)\right], \tag{6}$$

with $A = 0.111$, $\alpha = 2.254$, $\beta = 0.615$, and $B = 0.494$. At short distances ($R < R_1 = 5.0$ bohr radii), we extended the potential with an exponential wall of the form

$$V(R) = W \exp(-wR), \tag{7}$$

with

$$W = V(R)\exp(wR)|_{R_1}, \quad w = -\left.\frac{\partial \ln V(R)}{\partial R}\right|_{R_1}. \tag{8}$$

The two potential curves are shown in Fig. 1.

The phase shifts $\eta_l^{g,u}$ are determined from the continuum eigenfunctions $y_{E,l}^{g,u}(R)$, which are the regular solutions of the partial-wave equation

$$\left(\frac{d^2}{dR^2} + k^2 - \frac{2\mu}{\hbar^2} V_{g,u}(R) - \frac{l(l+1)}{R^2}\right) y_{E,l}^{g,u}(R) = 0. \tag{9}$$

The asymptotic form of $y_{E,l}^{g,u}(R)$ at large distances gives the elastic scattering phase shifts

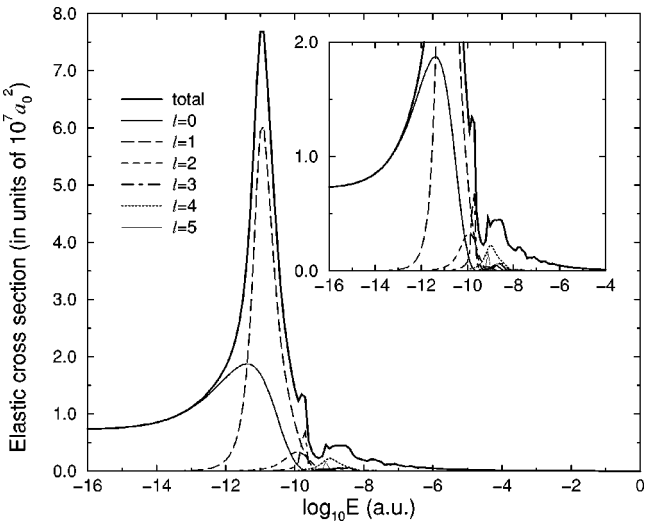

FIG. 2. Elastic cross sections for the $^2\Sigma_g^+$ state of Na_2^+.

$$y_{E,l}^{g,u}(R) \sim \sin\left[kR - \frac{l\pi}{2} + \eta_l^{g,u}(k)\right]. \tag{10}$$

III. ELASTIC CROSS SECTIONS

The elastic cross sections for the scattering at low energies in the $^2\Sigma_g^+$ and $^2\Sigma_u^+$ states are illustrated in Figs. 2 and 3, respectively. The insets in both figures have the same scale, contrary to the main plots. At very low energies below 10^{-12} a.u., the cross sections are determined by the *s* waves. The phase shifts may be described by the effective range formula [12]

$$k \cot \eta_0^{g,u}(k) = -\frac{1}{a_{g,u}} + \frac{\pi}{3}\frac{2\mu}{\hbar^2}\frac{C_4}{a_{g,u}^2}k + \frac{4}{3}\frac{2\mu}{\hbar^2}\frac{C_4}{a_{g,u}}k^2 \ln\left(\frac{k}{4}\sqrt{\frac{2\mu}{\hbar^2}C_4}\right) + \mathcal{O}(k^2). \tag{11}$$

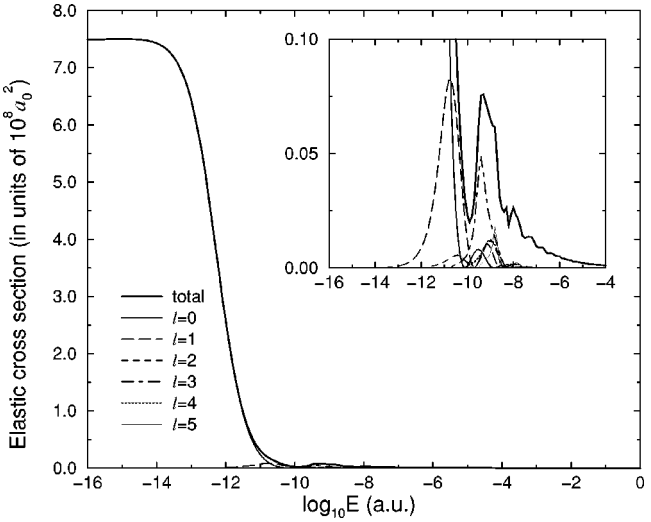

FIG. 3. Elastic cross sections for the $^2\Sigma_u^+$ state of Na_2^+.

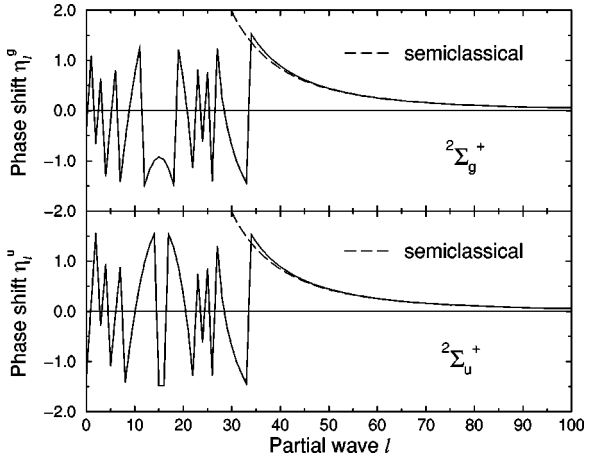

FIG. 4. Phase shifts for the gerade and ungerade states as a function of l for $E=10^{-6}$. The exact results are plotted between $-\pi/2$ and $\pi/2$.

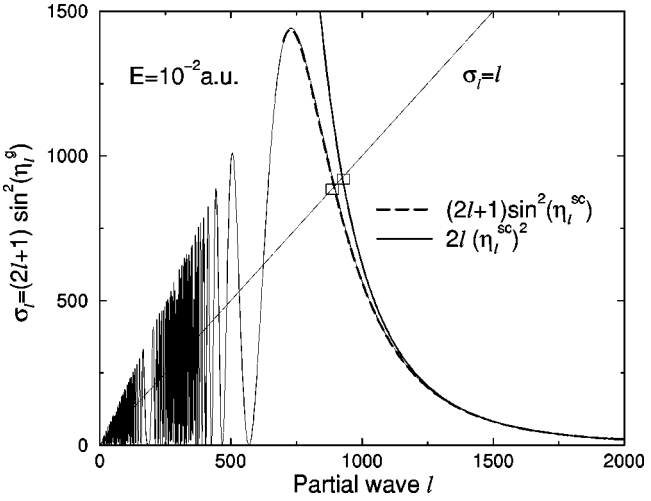

FIG. 5. Partial elastic cross section for the gerade state as a function of l for $E=10^{-2}$ a.u., and comparison with the semiclassical approximation for the phase shift η_l^{sc}, when considering $\sin\eta_l^{sc}$ or η_l^{sc}.

By fitting to the numerical data, we find the scattering lengths to be, in units of bohr radii a_0,

$$a_g = 763.3 a_0 , \tag{12}$$

$$a_u = 7721.4 a_0 . \tag{13}$$

The zero-energy cross sections are $\sigma_{\text{el.}}^g = 4\pi a_g^2 = 7.3\times 10^6 a_0^2 = 2.0\times 10^{-10}$ cm^2 for the $^2\Sigma_g^+$ state and $\sigma_{\text{elas.}}^u = 4\pi a_u^2 = 7.5\times 10^8 a_0^2 = 2.1\times 10^{-8}$ cm^2 for the $^2\Sigma_u^+$ state. The average is 1.1×10^{-8} cm^2.

Above 10^{-12} a.u., higher partial waves contribute, shape resonances occur, and considerable structure is present in the cross sections. For large values of the angular-momentum quantum number l, the centrifugal barrier ensures that the effect of the inner part of the potential is negligible, and the phase shifts are determined by the long-range interactions. For large l, we can use the semiclassical approximation for the phase shift [13]

$$\eta_l \simeq -\frac{\mu}{\hbar^2}\int_{R_0}^{\infty} dR \frac{V(R)}{\sqrt{k^2-(l+\frac{1}{2})^2/R^2}}, \tag{14}$$

where R_0 is the outer classical turning point. If R_0 is in the asymptotic region, so that $V(R)\sim -C_4/2R^4$, the phase shift is given by the simple expression

$$\eta_l^{g,u} \simeq \frac{\pi\mu^2 C_4}{4\hbar^4}\frac{E}{l^3}. \tag{15}$$

In Fig. 4 we show the numerical phase shifts (modulo π) for the gerade and ungerade states as functions of l for a collision energy of $E=10^{-6}$ a.u., and we compare them to the approximate semiclassical phase shifts. In both cases, the approximation is good for $l>50$: the lower partial waves for which the phase shifts are large cannot be described by this simple approximation.

A useful approximation to the cross section at energies where numerous phase shifts contribute can be obtained by dividing the individual partial waves at $l=L$ where L is large enough that the asymptotic expression (15) is valid and $\sin\eta_l$ may be approximated by η_l. If L is also such that the phase shifts quickly become large as l decreases below L, $\sin^2\eta_l$ may be replaced by its average value of 1/2. Then, it may be shown that

$$\sigma_{\text{el.}}(E) \simeq \frac{2\pi}{k^2}L^2 + \frac{4\pi}{k^2}\int_L^{\infty} dl\, 2l\, \eta_l^2 ,$$

$$\simeq \frac{2\pi}{k^2}L^2[1+\eta_L^2]. \tag{16}$$

A reasonable choice for L is such that $\eta_L=\pi/4$ (or $\sin^2\eta_L=1/2$, see Fig. 5). Then,

$$L = \left(\frac{\pi}{4}\frac{\mu^2 C_4}{\hbar^4}\frac{E}{\eta_L}\right)^{1/3} = \left(\frac{\mu^2 C_4}{\hbar^4}E\right)^{1/3} \tag{17}$$

and

$$\sigma_{\text{el.}}(E) = \pi\left(\frac{\mu C_4^2}{\hbar^2}\right)^{1/3}\left(1+\frac{\pi^2}{16}\right)E^{-1/3}. \tag{18}$$

For Na^+-Na, with E measured in atomic units,

$$\sigma_{\text{el.}}(E) = 4174 E^{-1/3} \text{ a.u.} \tag{19}$$

In Fig. 6 we compare the quantal elastic cross sections with the semiclassical expression as a function of the collision energy. The approximation gives results in good agreement with the exact ones for energies down to 10^{-10} a.u. At lower energies, the few partial waves contributing imply classical turning points R_0 where the approximation for the

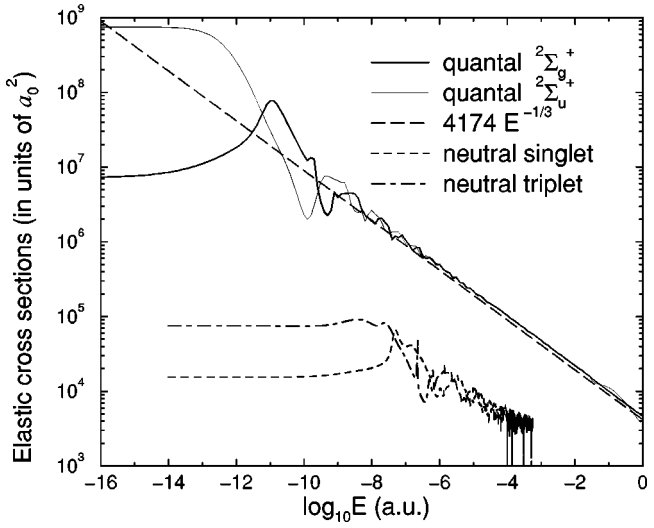

FIG. 6. Elastic cross sections as a function of the collision energy: comparison of the quantal and semi classical treatments, and the neutral singlet and triplet values from [14].

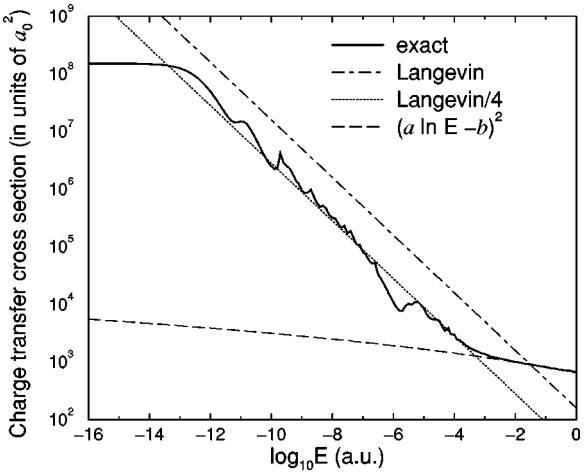

FIG. 7. Charge-transfer cross section as a function of the collision energy. The Langevin cross section and a fit given by $\sigma_{\text{Langevin}}/4$ are also shown.

phase shift cannot be used. At higher energies, the quantal results oscillate about the semiclassical one. On the same graph, we show the elastic cross sections for the collision of neutral sodium atoms in the $3s$ state in the molecular singlet $X\ ^1\Sigma_g^+$ and triplet $a\ ^3\Sigma_u^+$ states [14]. The cross sections of the atom-ion collisions are orders of magnitude larger than their neutral counterparts.

IV. CHARGE TRANSFER AND DIFFUSION CROSS SECTIONS

The charge-transfer cross section in the collision of Na^+ with Na is given by Eq. (3). In Fig. 7 we show it as a function of the collision energy. At high energies, the influence of the long-range attractive force tends to cancel and the cross section is determined by the exponential decay of the difference between the $^2\Sigma_g^+$ and $^2\Sigma_u^+$ potentials. The charge-transfer cross section varies as [7,13]

$$\sigma_{\text{ch}} \sim (a \ln E - b)^2 \text{ a.u.}, \tag{20}$$

with $a=1.33$, $b=22.943$, and E is expressed in eV. At high energies beyond our calculations, oscillations about the mean value have been predicted [15] and observed [16].

At low energies below 10^{-3} a.u., the cross section is dominated by scattering from the attractive $^2\Sigma_g^+$ interaction varying as R^{-4} and small values of the angular momentum. As shown in the figure, the cross section varies approximately as the classical Langevin formula for a polarization potential

$$\sigma_{\text{Langevin}} \sim \pi \sqrt{2C_4} E^{-1/2} \text{ a.u.} \tag{21}$$

modified by quantum oscillations. In the limit of zero energy, only the s-wave contributes and the Langevin formula fails. The limiting charge-transfer cross section is given by

$$\sigma_{\text{ch}} = \pi (a_g - a_u)^2 = 1.5 \times 10^8 a_0^2 = 4.2 \times 10^{-9} \text{ cm}^2. \tag{22}$$

For bosons, the diffusion cross section for an ion in its parent species is given by [13]

$$\sigma_d \equiv \frac{s+1}{2s+1}\sigma^+ + \frac{s}{2s+1}\sigma^-, \tag{23}$$

where $s=3/2$ is the nuclear spin of the Na atom, and

$$\sigma^+ = \frac{4\pi}{k^2}\left[\sum_{l\ \text{even}}^{\infty}(l+1)\sin^2(\eta_l^g - \eta_{l+1}^u) + \sum_{l\ \text{odd}}^{\infty}(l+1)\sin^2(\eta_l^u - \eta_{l+1}^g)\right] \tag{24}$$

and

$$\sigma^- = \frac{4\pi}{k^2}\left[\sum_{l\ \text{even}}^{\infty}(l+1)\sin^2(\eta_l^u - \eta_{l+1}^g) + \sum_{l\ \text{odd}}^{\infty}(l+1)\sin^2(\eta_l^g - \eta_{l+1}^u)\right]. \tag{25}$$

For large l, $\eta_l^{g,u} \simeq \eta_{l+1}^{g,u}$ and [13]

$$\sigma_d \simeq 2\sigma_{\text{ch}}. \tag{26}$$

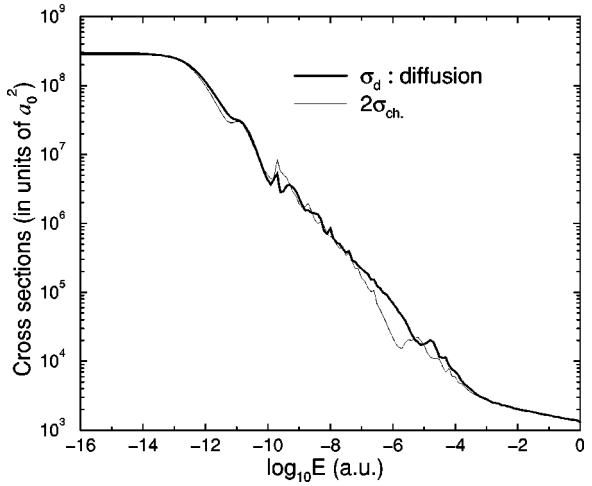

FIG. 8. Diffusion cross section as a function of the collision energy.

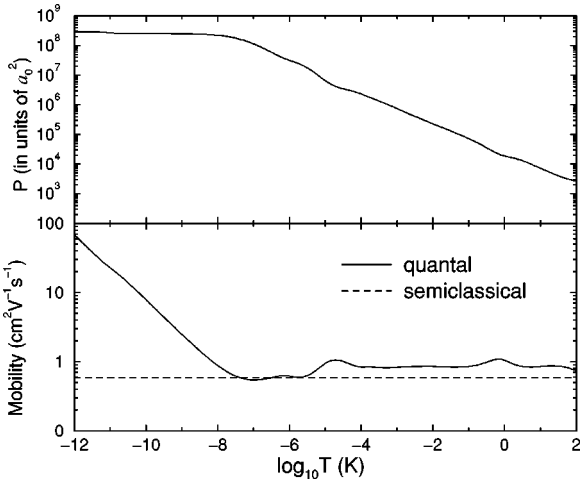

FIG. 9. Averaged diffusion cross section and ion mobility as functions of temperature.

In Fig. 8 we illustrate the diffusion cross section as a function of the collision energy, and compare it to twice the charge-transfer cross section. The agreement is close.

Using the diffusion cross section, we can calculate the ion mobility. The mobility of an ion is given by [7,13]

$$K=\frac{eD}{k_BT}, \tag{27}$$

where e is the charge of the ion, T the temperature, and D the diffusion coefficient which may be written as

$$D=\frac{3\sqrt{\pi}}{16(n_{\rm ion}+n)}\sqrt{\frac{2k_BT}{\mu}}\frac{1}{P}$$
$$\simeq\frac{3\sqrt{\pi}}{16n}\sqrt{\frac{2k_BT}{\mu}}\frac{1}{P}, \tag{28}$$

where n, the neutral gas density, is supposed much larger than the ion density $n_{\rm ion}$, and P is an averaged diffusion cross section given by

$$P=\frac{1}{2}\int_0^\infty dx\,x^2\exp(-x)\sigma_d(x), \tag{29}$$

where $x=E/k_BT$. If the scattering is described classically, the mobility corresponding to a R^{-4} potential of an ion of mass M (in units of proton mass) in its parent with a standard density $n=2.69\times10^{19}$ cm^{-3} is given by

$$K\simeq\frac{35.9}{\sqrt{MC_4}}\ \text{cm}^2\,\text{V}^{-1}\,\text{s}^{-1}, \tag{30}$$

where C_4 is in atomic units [13]. In Fig. 9 we show the averaged diffusion cross section and the ion mobility as functions of the temperature. The semiclassical expression (30) is valid over a large range of temperatures, from 10 nK to 100 K. At very low temperatures, the mobility increases rapidly as the averaged diffusion cross section reaches a plateau. At high temperatures, the mobility will ultimately decrease [7].

V. CONCLUSION

We have explored the scattering properties of collisions between a neutral atom and its positive ion, and calculated cross sections for Na and Na^+. The conclusions reached here are applicable to the other alkali-metal atom-ion collisions, since their interaction potentials are similar, and the results are well described by a semiclassical treatment, which depends only on the mass and polarizability of the neutral atom.

We showed that the elastic cross sections for the gerade and ungerade states are satisfactorily described by a simple semiclassical treatment to energies down to $E\sim10^{-12}$ a.u., for which they follow a $E^{-1/3}$ power-law dependence. The s-wave regime is not accessible with present day technology. The elastic cross sections are very large at low collision energies, of the order of $10^7a_0^2=2.8\times10^{-10}$ cm^2 for energies corresponding to 100 μK. They are two to three orders of magnitude larger than the elastic cross sections of two neutral sodium atoms.

The charge-transfer cross sections are very large at low collision energies. They are well described by the Langevin cross-section behavior $E^{-1/2}$ for E between 10^{-12} to 10^{-3} a.u., and vary as $(a\ln E-b)^2$ at larger energies. The large transfer cross section at low energy may provide ion cooling through collisions with ultracold neutral gas.

We verified the relationship $\sigma_d\simeq2\sigma_{\rm ch}$, and computed the ion mobility. For a large range of temperatures, from 10 nK to 100 K, it is almost constant and agrees with the classical formula for a polarization potential. At low temperatures, the calculated mobility increases as $1/T$ as the temperature is decreased.

However, at ultralow temperatures, many-body interactions become important and the behavior of the system cannot be described in terms of binary collisions. In that regime,

the ultracold atoms form a frozen gas similar to an amorphous glass where the sites are randomly distributed over the sample. In such a disordered system, charge hopping can occur due to many-body effects, and insulator-conductor transitions can take place. Similar many-body effects have been observed in excitation transfer in a frozen gas of ultracold Rydberg atoms [17]. Ultracold atom-ion collisions may provide a useful laboratory to study many-body effects, like Mott transitions, in very clean experimental systems.

ACKNOWLEDGMENTS

The authors would like to thank W.W. Smith for discussions of ion-atom collisions at ultracold temperatures. R.C. is supported by the National Science Foundation through Grant No. PHY-9970757. A.D. acknowledges the support of the Division of Chemical Sciences, Office of Basic Energy Sciences, U.S. Department of Energy.

[1] J. Weiner *et al.*, Rev. Mod. Phys. **71**, 1 (1999); R. Côté and A. Dalgarno, Phys. Rev. A **58**, 498 (1998).
[2] A. Fioretti *et al.*, Phys. Rev. Lett. **80**, 4402 (1998); T. Takekoshi, B.M. Patterson, and R.J. Knize, *ibid.* **81**, 5109 (1998); A.N. Nikolov *et al.*, *ibid.* **82**, 703 (1999); N. Balakrishnan, R.C. Forrey, and A. Dalgarno, *ibid.* **80**, 3224 (1998).
[3] W.C. Stwalley and H. Wang, J. Mol. Spectrosc. **195**, 194 (1999); R. Côté and A. Dalgarno, *ibid.* **195**, 236 (1999); R. Côté *et al.*, Phys. Rev. Lett. **74**, 3581 (1995).
[4] K.B. Davis *et al.*, Phys. Rev. Lett. **75**, 3969 (1995); M.H. Anderson *et al.*, Science **269**, 198 (1995); C.C. Bradley *et al.*, Phys. Rev. Lett. **75**, 1687 (1995); D.G. Fried *et al.*, *ibid.* **81**, 3811 (1998).
[5] T.C. Killian *et al.*, Phys. Rev. Lett. **83**, 4776 (1999).
[6] P.L. Gould and E.E. Eyler (private communication).
[7] E.W. McDaniel, *Collision Phenomena in Ionized Gases*, 1st ed. (Wiley, New York, 1964).
[8] S. Magnier, Ph.D. thesis, University of Paris, Orsay, France, 1993 (unpublished).
[9] C.R. Ekstrom *et al.*, Phys. Rev. A **51**, 3883 (1996).
[10] J. Tharamel, Ph.D. thesis, University of New Hampshire, Durham, 1995 (unpublished).
[11] J.N. Bardsley *et al.*, Phys. Rev. A **11**, 1911 (1975).
[12] T.F. O'Malley, L. Spruch, and L. Rosenberg, J. Math. Phys. **2**, 491 (1961).
[13] A. Dalgarno, M.R.C. McDowell, and A. Williams, Philos. Trans. R. Soc. London, Ser. A **250**, 411 (1958); A. Dalgarno, *ibid.* **250**, 426 (1958).
[14] R. Côté and A. Dalgarno, Phys. Rev. A **50**, 4827 (1994).
[15] C. Bottcher, A.C. Allison, and A. Dalgarno, Chem. Phys. Lett. **11**, 307 (1971); J. Tharamel, V.A. Kharchenko, and A. Dalgarno, Phys. Rev. A **50**, 496 (1994).
[16] J. Perel *et al.*, Phys. Rev. Lett. **23**, 677 (1969); J. Perel *et al.*, Phys. Rev. A **1**, 1626 (1970); H. L. Daley and J. Perel, *Abstracts of the 6th International Conference on the Physics of Electronic and Atomic Collisions* (MIT Press, Cambridge, 1969), p. 1051.
[17] W.R. Anderson, J.R. Veale, and T.F. Gallagher, Phys. Rev. Lett. **80**, 249 (1998); I. Mourachko *et al.*, **80**, 253 (1998).